Measurement of Stark Profiles of the Lyman-α and Lyman-β Lines of Hydrogen in an Electromagnetic Shock Tube*

R. C. ELTON†
U. S. Naval Research Laboratory, Washington, D. C.

AND

H. R. GRIEM
University of Maryland, College Park, Maryland
and
U. S. Naval Research Laboratory, Washington, D. C.

(Received 9 April 1964)

Measurements in the vacuum ultraviolet spectral region of optically thin (except in narrow wavelength bands in the line cores) profiles of the Stark-broadened Lyman-α and Lyman-β lines of hydrogen (0.03% admixture in 40 mm Hg helium) agreed to within 10% with Stark-broadening theory over three and two decades of intensity, respectively. A shot-to-shot scan technique was employed, using a highly reproducible T-type electromagnetic shock tube. The present theoretical line-broadening calculations include both the effects of quastistatic ion microfields and those of electron impacts, whereas the Holtsmark theory neglects the electrons and differs by a factor of 2–3 on the far wings (depending upon the normalization). A peak temperature of 20 500°K (±8%) was determined spectroscopically from the helium line-to-continuum intensity ratio and was consistent with the hydrodynamic temperature obtained from shock-velocity measurements. A charged-particle density of a few times 10^{17} cm^{-3}, used in comparing the measured profiles with theory, was obtained from the visible continuum intensity and agreed with hydrodynamic predictions, as well as with half-width measurements of neutral helium lines in the visible region.

INTRODUCTION

THE Stark effects caused by electric fields of ions and electrons in a plasma constitute the most important mechanism for pressure broadening of spectral lines in stellar atmospheres and interiors and also in many laboratory experiments with arcs, shock tubes, and various other plasma sources. Since Stark broadening is insensitive to temperature, measurements of line profiles emitted from optically thin layers yield directly charged-particle densities. In optically thick layers, the radiative energy transport in a given line is determined by both the broadening mechanism and the line strength. However, for both optically thick and thin lines heavy reliance must be placed upon the theory to obtain densities.

The theory is complicated by the fact that the characteristic frequencies associated with the electron microfields are often comparable to the frequency separation of the energy levels or even larger. Therefore, deviations from adiabaticity (the inclusion of inelastic scattering) in the time development of the wave functions for the emitting atom and interference effects caused by overlapping lines had to be taken into account. However, due to the high velocities of electrons, their effects could usually be calculated in the impact approximation, in which details of the time development during individual collisions are not required but rather only the connection between wave functions before and after many weak collisions. The resulting profiles are then of a dispersion type in case of isolated lines, or are superpositions of such dispersion profiles with additional interference terms whenever lines overlap. (Details of these theoretical considerations are summarized in a recent review article.[1]) The statistical treatment of the broadening by ions, corresponding to the quasistatic approximation due to Holtsmark,[2] was considerably simpler because the ion velocity could normally be neglected. Here the perturbing ions were assumed to be independent particles; however, ion-ion correlations and Debye shielding of the ion fields by electrons influence the central region of the profile and must also be included in a complete theory.[3]

In general, one-electron spectra are most suitable for the verification of line-broadening theory since the unperturbed wave functions are known exactly, thus eliminating one source of uncertainty. For such lines electron and ion broadening are comparable because there is a first-order Stark effect in static fields due to the degeneracy. However, the various corrections (electron impacts, correlations, shielding) to the original Holtsmark profiles tend to compensate each other in the case of the Balmer lines; e.g., the half-width of the most extensively studied Hβ line is given quite accurately by the Holtsmark theory. This renders such lines rather insensitive to theoretical details and it is difficult to separate the ion and electron effects from a composite profile. The impressive body of experi-

* Jointly sponsored by the National Science Foundation and the National Aeronautics and Space Administration.

† Some of the material in this article is part of a thesis (see also footnote 10) submitted in partial fulfillment of the requirements for the degree of Doctor of Philosophy at the University of Maryland, College Park, Maryland, 1963.

[1] M. Baranger, *Atomic and Molecular Processes*, edited by D. R. Bates (Academic Press Inc., New York, 1962), Chap. 13.
[2] J. Holtsmark, Ann. Physik 58, 577 (1919).
[3] B. Mozer and M. Baranger, Phys. Rev. 118, 626 (1960).

mental information[1,4] therefore mainly confirms the over-all accuracy of electron and ion Stark-broadening calculations for hydrogen and ionized helium or, in the case of isolated lines from two or more electron systems, the joint accuracy of Stark-broadening theory and approximate atomic matrix elements.

The Lyman-α line constitutes an almost ideal test case for the theory of electron broadening; two-thirds of its intensity is in the components which are not shifted by the static-ion fields and are therefore affected only by electron impacts. The predicted deviations from the Holtsmark profile are, accordingly, larger for Lyman-α than for the other hydrogen lines normally observed. Another advantage is the possibility of obtaining large variations in the relative intensity with small changes in wavelength on scanning over the line. This minimizes asymmetries in the line profile,[4] which were not included in the calculations.[5] For example, the variation in photon energy across the profile remains small compared to thermal energies ($h\Delta\nu/kT\approx\pm 0.05$ in the present experiment) so that variations in the Boltzmann factors can be neglected. To cover the same intensity range on the profile of the Hβ line, much larger values of $\Delta\nu/\nu$ and $h\Delta\nu/kT$ are encountered on the extreme wings.

Corrections to the Holtsmark profile due to electron impacts become much smaller for the Lyman-β line because there are no unshifted central components. However, near the line center its profile depends quite critically on the quasistatic-ion broadening, and a reliable measurement in the region of the predicted central dip could serve to verify the accuracy of the recently derived ion field-strength distribution functions used in the calculations. However, because of difficulties with self-absorption, such measurements proved to be impractical. Self-absorption, especially in cooler layers between the main body of the plasma and the vacuum spectrograph slit, is even more pronounced for the stronger Lyman-α line with its predicted sharp central peak. This has made it impossible to check the theory in the cores of the lines. Therefore, measurements of visible (nonresonance) lines lead to a better comparison with the theory of the central core. In this respect, the experiment described in this paper is complementary to previous measurements of other lines, i.e., it should mainly be expected to yield information on the electron contribution to the wing broadening, which is of greatest interest in astrophysical and radiative transfer applications where the equivalent width of a self-absorbed line is determined mainly by the wing distribution of the adsorption coefficient.

Besides the difficulties with self-absorption, some of the theoretical advantages in studying the Lyman-α line could also be lost by the increased experimental errors inherent in vacuum-spectroscopy investigations. To minimize these errors, both the plasma-light source and detecting apparatus had to be specially designed. Of the more common plasma-light sources, namely arcs and shock tubes, the choice fell upon the latter since it promised to produce a relatively homogeneous and optically thin plasma with a minimal cool boundary layer (in which self-absorption could be serious) and a high enough charged-particle density so that Stark broadening of the lines would dominate.

Another reason for working at high-electron densities is that only then may local thermodynamic equilibrium be expected to hold, i.e., collisional processes dominate radiative processes so that excited-state population numbers and the degree of ionization can then be calculated from the Saha-Boltzmann equations. This equilibrium greatly facilitates the spectroscopic determination of plasma conditions required for the computation of theoretical profiles, but it is otherwise not too essential because Stark broadening is not very sensitive to details in the velocity distributions of the perturbing particles, or even their mean velocities. Still, the electron densities are high enough and temporal changes in macroscopic plasma paramenters are sufficiently slow so that local thermodynamic equilibrium in the test plasma should be attained with very good precision (within $\sim 5\%$ in terms of population densities of excited states) at any instant of time. This follows from theoretical estimates[6] of deviations from such equilibrium due to radiative decay or recombination which are not balanced by photoexcitation or ionization. The deviations of the population density ratios between excited, bound, or free states are much smaller, i.e., completely negligible. Only these relative densities enter into the various spectroscopic relations used in the analysis of the measurements, an exception being the calculated blackbody saturation limits in optically thick regions of the line profiles.

SHOCK TUBE APPARATUS AND EXPLORATORY EXPERIMENTS

The charged-particle density required to sufficiently broaden the hydrogen resonance lines for accurate measurement was obtained in a partially ionized helium plasma behind a reflected shock wave generated in a T-type electromagnetic shock tube. By operating at an abnormally high initial pressure (40 mm Hg) and aspect ratio (75 cm long and 24 mm inside diameter), extremely reproducible conditions were obtained with a low-impurity level and consequent spectroscopic purity.

Nickel electrodes (which do not produce lines near Lyman-α and Lyman-β) spaced 25 mm apart were sealed to the ends of the short section of the quartz T-tube with O-rings (Fig. 1) and were further cushioned with a second pair of split O-rings inside the tube. Of

[4] H. R. Griem, *Plasma Spectroscopy* (McGraw-Hill Book Company, Inc., New York, 1964).

[5] H. R. Griem, A. C. Kolb, and K. Y. Shen, Phys. Rev. **116**, 4 (1959); see also U. S. Naval Research Laboratory Reports NRL 5455, 1960, and NRL 5805, 1962 (unpublished).

[6] H. R. Griem, Phys. Rev. **131**, 1170 (1963).

the many insulating materials tried in the construction of the shock tube, only 3-mm wall thickness quartz tubing withstood the high-thermal shock for a reasonable number of shots. Pyrex, for example, developed severe microcracks due to the rapid heat-cool cycle on each shot and broke after a few discharges under these conditions. A current reaching a peak of 5×10^5 A in 3 μsec was produced by a capacitor bank of 108 μF charged to 8100 V. The external circuit resistance was 0.003 Ω and the shock tube resistance 0.008 Ω so that the discharge was strongly damped, with $\sim$60% of the available energy deposited during the first half-cycle.

A preliminary parametric study of plasma conditions in the shock tube was carried out using a Zeiss stigmatic quartz spectrograph for space-resolved studies along the major axis of the tube, a rotating-drum optical spectrograph[7] with 0.5-μsec time resolution, and a $f/2.9$ rotating-mirror streak camera[8] which could resolve 0.1 μsec signals. By varying the pressure, voltage, and tube length it was determined that a sufficiently long tube resulted in a gradual separation of three zones (somewhat analogous to that observed in conventional shock tube studies): (a) a nonluminous relaxation zone behind the incident shock front followed after a few microseconds by (b) a luminous zone and later by (c) an impurity-laden zone with an associated high intensity (Fig. 2). Both the time-resolved and the space-resolved time-integrated spectrograms (Fig. 3) indicated that the end of the shock tube remained free of impurity radiation, in contrast to the highly contaminated region further down the tube. Streak photographs taken with color film also showed that the reflected shock wave is quite effective in suppressing the flow of impurity-dominated plasma which follows behind the incident luminous wave up the tube, resulting in a spectroscopically pure region extending about 5 cm from the reflector. Such a condition is most desirable in an experiment such as this where up to 100 consecutive discharges are required without appreciable window fogging due to deposition of impurities at the point of observation.

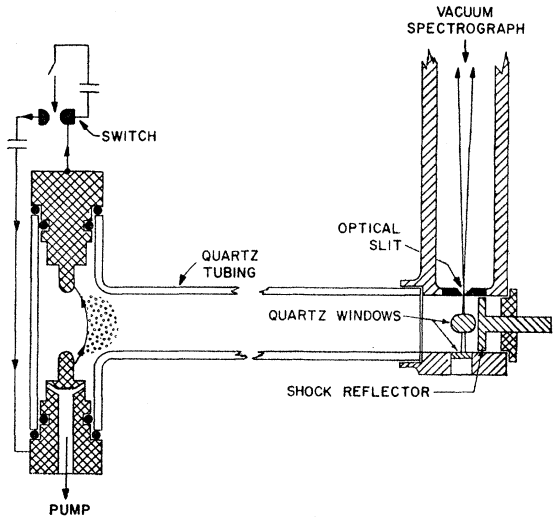

FIG. 1. Schematic diagram of the shock tube and the vacuum spectrograph adapter with the slit at the plasma boundary. The adjustable reflector is shown at the tube end.

[7] G. G. Milne, University of Rochester Institute of Optics, (unpublished).

[8] F. L. Brauer and D. F. Hansen, J. Opt. Soc. Am. 49, 421 (1959).

The background hydrogen concentration (without deliberately adding hydrogen) was obtained with a Bausch and Lomb 50-cm grating monochromator which photoelectrically monitored the variation in the Hα intensity as known amounts of hydrogen were added to the initial helium filling. The intensity-concentration data were extrapolated to measure the background hydrogen. In tubes just short enough (50 cm long) to show no separation between the incident shock wave and the first luminous zone there existed $\sim$0.4 mm Hg equivalent hydrogen in the tube initially. However, in using somewhat longer tubes (75 cm), such that a significant separation developed behind the incident shock wave and the first luminous zone, the reflected shock contained only 0.015 mm Hg equivalent initial hydrogen. Since a low-hydrogen content was essential in obtaining optically thin radiation close to the center of the resonance lines, the slightly reduced shock strength associated with the longer tubes was accepted. A mass spectrometer analysis of the spectroscopically pure fill gas showed a hydrogen background of less than 4 ppm. Thus, it was concluded that the 0.015 mm Hg measured was due to wall adsorption of hydrogen. An interesting and essential point is that the hydrogen concentration remained constant to within 10% over a series of 100 shots, after a few initial discharge-cleaning shots, suggesting that a surface-adsorption saturation condition[9] existed.

In addition to the Bausch and Lomb scanning monochromator mentioned above, which was also used as a temperature monitor, a Leiss double-prism monochromator was used to observe the absolute continuum radiation in an 80-Å interval near 5414 Å as a measure of the electron density on each shot. Absolute calibration of this instrument was obtained by an *in situ* comparison against a tungsten-ribbon standard lamp.[10,11] All spectroscopic observations were simultaneously carried out on the reflected shock wave at a distance of 3 mm from the reflector.

APPARATUS FOR THE LINE-PROFILE MEASUREMENTS

The vacuum ultraviolet spectroscopy was performed with a McPherson 2.2-m normal incidence spectro-

[9] J. H. Leck, *Advances in Mass Spectrometry* (Pergamon Press, Inc., New York, 1959).

[10] R. C. Elton, U. S. Naval Research Laboratory Report NRL 5967, 1963 (unpublished).

[11] E. A. McLean, C. E. Faneuff, A. C. Kolb, and H. R. Griem, Phys. Fluids 3, 843 (1960).

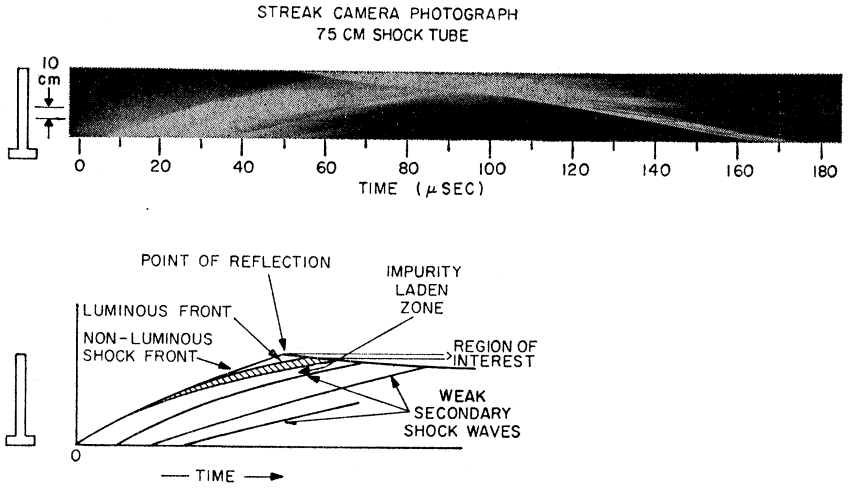

FIG. 2. Typical streak camera photograph of a portion of the 75-cm shock tube with the camera slit imaged parallel to the tube axis. The lower diagram identifies features more apparent on the original negative and, in particular, on similar photographs taken in color, where a red luminous zone and reflected shock wave were quite distinct when compared to the cooler impurity region (white) behind the interface.

graph with a reciprocal dispersion of 3.75 Å/mm. No windows were used between the plasma and the spectrograph. While lithium fluoride does transmit in the Lyman-α region, the lower limit for transmission was found to shift from 1050 to 1400 Å after a few discharges, apparently due to surface damage of the window when placed adjacent to the plasma.[12] In order to avoid excessive self-absorption of the radiation by neutral hydrogen between the plasma and the spectrograph slit, the slit was shifted directly to the plasma by rebuilding the slit holder to incorporate the end section of the shock tube as shown in Fig. 1. Access ports were provided for viewing the plasma simultaneously through quartz windows with the optical monochromators. The vacuum spectrograph was powered through an isolation transformer to eliminate axial currents, which otherwise damage the slit and perturb the shock front. A special detector[13] relatively insensitive to radiation above 1350 Å was used for detection of the vacuum ultraviolet light pulses.

Since the line profiles were ultimately obtained by scanning the line in small wavelength increments between successive discharges, appreciable accuracy in the scanning mechanism was required. The instrument was equipped with a synchronous motor and associated gear system capable of defining successive 0.25-Å intervals with a standard deviation from the mean of 2% in incremental width. This result was obtained by scanning the steep portion of the wing of a spectral line from a steady source in increments of 0.25 Å and comparing with the profile obtained from a continous scan. The absolute wavelength calibration of the scanning mechanism was obtained by scanning between known lines using the same increments as for the Lyman line-profile scans.

Two dual-trace oscilloscopes were used to obtain the line profile and associated spectroscopic data. The electron density was monitored on one channel of each oscilloscope via the visible continuum radiation signal. The other channels monitored, respectively, an increment of the vacuum untraviolet hydrogen line and a helium line in the visible region, which was used in the temperature determination. The oscilloscope sweep was delayed for 40 μsec after the arc was initiated, which permitted the use of an expanded time scale (5 μsec/cm) for a detailed study of the time history of the signals. All data were read simultaneously at a time corresponding to a predetermined value of charged-particle density and the associated continuum signal.

SPECTROSCOPIC PLASMA ANALYSIS

Determinations of the charged-particle density and temperature were required for computing the theoretical line shapes, independently of the vacuum ultraviolet

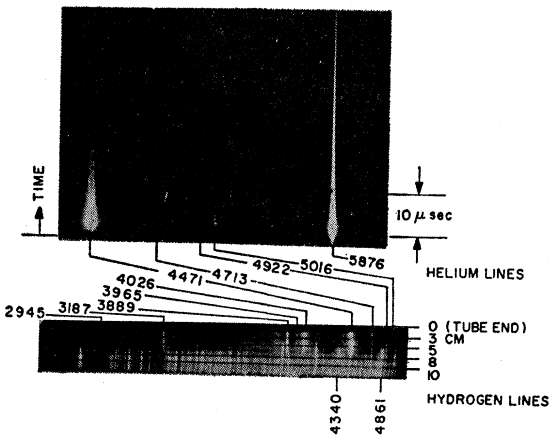

FIG. 3. Time-resolved (taken at 3 mm from reflector) and space-resolved (along the major axis) spectra. (Radiation from the first centimeter behind the reflector is obscured on the latter spectrum by the vacuum sealant.) The horizontal dark lines are reference marks on the tube. Both spectra were obtained on single shots.

[12] J. C. Boyce, Rev. Mod. Phys. 13, 1 (1941).
[13] R. Lincke and T. D. Wilkerson, Rev. Sci. Instr. 33, 911 (1962).

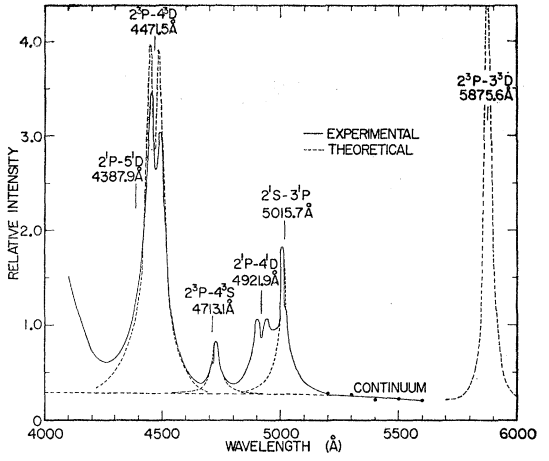

FIG. 4. Shot-to-shot photoelectric scan of a portion of the visible helium spectrum showing the overlapping lines, the continuum level, and the absorption effects ($N_e \approx 3.5\times10^{17}$ cm^{-3}, $T \approx 20\,000$°K).

observations. Stark profiles are mainly sensitive to the charged-particle density (the width is approximately proportional to $N_e^{2/3}$) and quite insensitive to temperature.[5] However, a reasonably accurate temperature determination was necessary for a self-consistent spectroscopic analysis of the plasma state and for comparison with the hydrodynamic data. In addition, a high shot-to-shot reproducibility in temperature was imperative to obtain accurate profile scans because the Lyman-α and Lyman-β line intensities are strong functions of temperature.

A charged-particle density determination independent of line broadening was obtained from an absolute measurement of the visible continuum radiation arising from free-free (bremsstrahlung) and free-bound (electron-ion radiative recombination) transitions. The theoretical continuum absorption coefficient is insensitive to temperature in the region of interest, i.e., around 20 000°K a 10% fluctuation in temperature corresponds to ~2% in density. Since in helium the excited states are nearly hydrogen-like, the hydrogenic approximation can be used for helium recombination cross sections with only slight corrections—particularly for wavelengths greater than 4000 Å where free-bound transitions to the $n=2$ level can be ignored. The hydrogenic approximation was corrected by employing exact helium energy levels $E_{n,l}$, effective quantum numbers n^* [defined by $(n^*)^2 = I_H/(I_{He}-E_{n,l})$, with I_H and I_{He} being the ionization potentials of hydrogen and helium, respectively], and hydrogen free-bound Gaunt factors $g_{fb}(n,l)$.[14] Recent quantum-defect calculations[4,15] of effective helium Gaunt factors yielded a helium continuum formula agreeing within a few percent with the former approach, well within the estimated accuracy of either method and of the measurements.

A shot-to-shot scan of the visible helium spectrum in the region of interest is shown in Fig. 4. Due to the overlapping of the helium lines at the high charged-particle density existing ($\sim3.5\times10^{17}$ cm^{-3}), continuum measurements were limited to an interval of about 400 Å as shown. A careful photoelectric scan of this region, as well as time and space resolved photographic spectrograms (Fig. 3), indicated that there existed no significant contribution to the continuum signals from impurity radiation. Small corrections to the continuum intensity due to the far wings of the helium lines were made using the line-broadening theory.[16] The continuum measurements of the charged-particle density yielded values with an accuracy of ±10%. As a check on the consistency of the data, theoretical profiles based upon this charged particle density were also calculated using the Stark-broadening theory for helium.[16] The resulting agreement (Fig. 4) with the measured line shapes added confidence in the continuum measurements of charge-particle density.

The ratio of the total intensity of a helium line to the underlying continuum is a function independent of electron density and strongly dependent upon temperature.[17,18] For example, in the 20 000°K region, a 10% measurement of this ratio yields a 3% temperature determination. The accuracy of this technique was somewhat limited by the overlapping of the visible lines. Thus, broadband measurements of the total line intensity of a particular helium line led to erroneous temperatures. Such measurements were, however, quite useful in monitoring temperature variations on each shot during a profile scan when they were "calibrated" against a more accurate temperature determination. This calibration was effected by carefully scanning the visible lines, such as in Fig. 4, with an instrumental resolution of 3 Å. The 4713-Å line was weak enough not to be seriously distorted by self-absorption and suffered least from overlap with adjacent lines. Detailed scans of this line were fitted with theoretical profiles calculated, using Stark-broadening theory,[16] for an electron-density value measured simultaneously from the visible continuum intensity. The ratio between the resulting total line intensity and the extrapolated underlying continuum intensity then yielded a peak

[14] W. J. Karzas and R. Latter, Astrophys. J. Suppl. No. 55, Vol. VI: 167 (1961).

[15] A. D. Anderson, and H. R. Griem, *Proceedings Sixth International Conference on Ionization Phenomena in Gases, Paris, 1963* (North-Holland Publishing Company, Amsterdam), Vol. III, p. 293.

[16] H. R. Griem, M. Baranger, A. C. Kolb, and G. Oertel, Phys. Rev. **125**, 177 (1962); see also H. R. Griem, *ibid.* **128**, 515 (1962).

[17] H. R. Griem, *Proceedings Fifth International Conference on Ionization Phenomena in Gases, Munich, 1961* (North-Holland Publishing Company, Amsterdam, 1962), Vol. II, p. 1856. The slight density dependence disappears if high-density corrections are introduced into the continuum formula as well [H. R. Griem, Phys. Rev. **128**, 997 (1962)].

[18] H. F. Berg, A. W. Ali, R. Lincke, and H. R. Griem, Phys. Rev. **125**, 199 (1962). The plot of line-to-continuum intensity versus temperature for the helium line at 5016 Å in Fig. 1 of this reference is erroneous and should be recalculated from basic formulas.

temperature of $(20.5\pm1.6)10^3$ °K. Similar measurements made on the 4471 and 5016 Å lines with slightly less precision afforded consistent results.

REPRODUCIBILITY AND HYDRODYNAMIC CONSIDERATIONS

Shot-to-shot fluctuations in the line-profile scans were kept to a minimum by reading all data at a time during the pulse corresponding to a specific value of the continuum signal. It was thus possible to maintain a shot-to-shot consistency in charged-particle density to better than 3%. Theory predicts for these conditions that a fluctuation of 7% in charge density is equivalent to a 1% fluctuation in temperature, which implies that the plasma temperature at the instant of analysis in this experiment should be reproducible to better than 0.5%. Since a 1% fluctuation in temperature corresponds, in the 1000-Å region, to a 5% fluctuation in blackbody intensity and as high as 10% in specific intensity on a line wing (due to the associated variation in charged-particle density) a small temperature fluctuation was a most important factor in obtaining reproducible signals for a line scan in the vacuum ultraviolet region.

Fortunately, it was possible to check the temperature stability since shock theory also predicts that the shock velocity should vary approximately as the temperature in this regime. By photoelectrically monitoring the transit time of the shock front from the electrode region to the end of the tube, shot-to-shot fluctuations in the average velocity of the shock wave were determined. Due to the very long tube used, it was thus possible to measure average velocity fluctuations to $\pm1\%$, whereas the absolute (spectroscopic) temperature measurement was only reliable to $\pm8\%$. The velocity fluctuations were consistent with expectations, i.e., they indeed indicated a temperature reproducibility of at least 1% from shot-to-shot, as did the vacuum ultraviolet intensity fluctuations. The large percentage of useful data (as discussed in the next section) may be due in part to the high degree of planarity for the reflected shock wave as evidenced by streak photographs taken with the slit of the camera imaged perpendicular to the axis of the shock tube, as well as by the close correspondence of simultaneous transverse spectroscopic measurements taken stereoscopically on each shot.

The relevance of the ideal Rankine-Hugoniot equations to the relation between the plasma state and velocity of shock waves generated in electrical shock tubes has been the subject of considerable discussion.[10,11,19–21] However, it is possible that the usual hydrodynamic theory is applicable for the present parameters. This follows because at the high initial pressures used here, precursor radiation has a small mean free path and also the excitation and ionization relaxation times behind the reflected shock are very short. As a check the instantaneous incident shock velocity near the reflector was measured from streak camera photographs (Fig. 2) by extrapolation of the shock front from the luminous region 50 cm from the electrodes to the point of reflection. The measurements yielded a velocity with a probable error of $\pm5\%$, a corresponding temperature to $\pm5\%$, and a charged-particle density to $\pm35\%$, with error brackets overlapping those of the spectroscopic measurements of these parameters which in the case of the electron density are more precise ($\pm10\%$). Better velocity measurements near the end of the tube are required to make a more precise comparison.

LYMAN-α LINE-PROFILE DETERMINATION

The Lyman-α profile data was obtained by scanning the line in discrete steps, with repetitive measurements in regions of the profile that were critical to the theoretical comparison. Since the quartz shock tubes did not last more than about 100 shots unless cleaned and refired to remove crazing effects, only rough scans were made over the entire profile from one far wing to the other. These preliminary scans, as well as some time-integrated profiles obtained on film, indicated some interference from Si III lines on the short-wavelength wing of the Lyman-α line.[22] Also, the presence of a slight asymmetry in the reabsorption dip in this line, to be discussed later, indicated that measurements on the long-wavelength wing could probably be extended further towards the core of the line. Final precise scans were therefore begun at about 2 Å from the line center on the short-wavelength wing and continued towards longer wavelengths.

The raw data for each wavelength interval of a Lyman-α scan, with background hydrogen concentration equivalent to 0.015 mm Hg initial pressure, is shown in Fig. 5 (lower curve). Narrowband reabsorption in the cooler regions near the walls was suspected as the cause of the central dip in the Lyman-α profile. If this assumption were valid, the signal level in the dip should essentially depend only upon the boundary-layer temperature and should be insensitive to small changes in hydrogen concentration. Also, the signal level outside of the central region should exhibit a linear dependence upon hydrogen concentration as long as the plasma conditions are not perturbed by the additional hydrogen and as long as the blackbody limit is not approached in the emitting plasma. To check these hypotheses, hydrogen was added in known amounts and measurements were made at 1 and 4 Å from the line center and throughout the central dip

[19] W. Wiese, H. F. Berg, and H. R. Griem, Phys. Rev. **120**, 1079 (1960).
[20] W. Wiese, H. F. Berg, and H. R. Griem, Phys. Fluids **4**, 250 (1961).
[21] M. Cloupeau, Phys. Fluids **6**, 679 (1963).

[22] The He II line at 1215.2 Å was estimated to be $\sim10^{-5}$ times the intensity of Lyman-α and was therefore negligible.

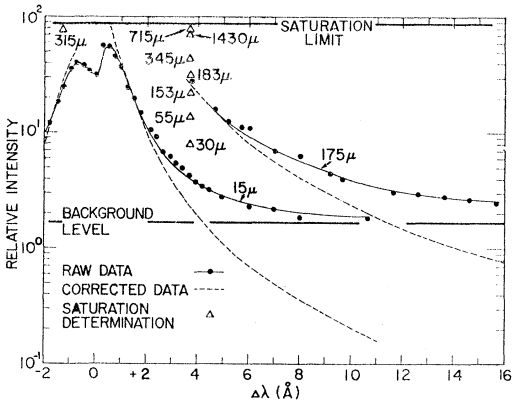

FIG. 5. Data for the Lyman-α Stark profile. The equivalent hydrogen pressures are in microns of mercury ($N_e=3.3\times10^{17}$ cm^{-3}, $T\approx20\,000$°K).

region. No effect was observed on the central signal, whereas the signal at 1 Å did rise, but saturated very quickly with less than 1% added hydrogen. At 4 Å the signal did rise linearly with total hydrogen concentration, eventually saturating at the same level as the 1-Å signal, and finally fell off as the plasma temperature decayed with further increased hydrogen concentration (for greater than about 3% hydrogen). A similar decrease at high concentrations was observed for the Hα line. These observations follow at least qualitatively the behavior predicted by hydrodynamic theory[23] with various hydrogen-rare gas mixtures.

As described earlier, a downward extrapolation of the concentration curve obtained in the optically thin region at 4 Å from line center afforded an estimate of the background hydrogen concentration ($\sim$0.015 mm Hg), while a fit of the high-concentration nonlinear portion with a function of the form $1-\exp(-\tau)$, where τ is the optical depth (absorption coefficient times the depth of the plasma), gave an estimate of the blackbody limit. Complete (i.e., both wings) profiles of Lyman-α and Lyman-β at a high concentration of hydrogen yielded a flat top over a wavelength spread of ±5 Å from center (except, of course, at the line center) within the usual shot-to-shot data fluctuation of $\sim5\%$. This result supports the existence of a well-defined blackbody limit. The flat top is also further evidence that the source is homogeneous, since the optical depth depends upon the wavelength.

For wavelength displacements from line center greater than 6 Å the Lyman-α wing signal approached that of the background level (Fig. 5) and consequently the estimated uncertainty incurred in reading the signal resulted in a large uncertainty in the true wing intensity as shown in Fig. 7. In an effort to reduce this effect and to extend the profile determination as far as possible, a second wing profile was begun at 4 Å from line center and extended to 16 Å with a hydrogen admixture of 0.175 mm Hg maintained. The results are shown in the upper curves in Figs. 5 and 7.

[23] E. B. Turner, U. S. Air Force Office of Scientific Research Contract No. AFOSR TN 56-150, DDC Document No. AD 86309, 1956 (unpublished).

CORRECTIONS TO THE LYMAN-α PROFILE

Based upon the above evidence, corrections for self-absorption were applied to the points near the line center by inserting the optical depth τ_λ derived from the measured emissivity $\epsilon_\lambda=I_\lambda/B_\lambda=1-\exp(-\tau_\lambda)$ into the solution of the radiative transfer equation for the case of an optically thin plasma $I_\lambda'=\tau_\lambda B_\lambda$ assuming a uniform slab of radiating plasma. (Here I_λ is the measured spectral intensity and B_λ is the Planck function.) The corrected data is shown dashed in Fig. 5 for displacements from the line center of less than ±1.5 Å. A reasonable estimate for the accuracy of the measured blackbody signal level is 10%, corresponding to an uncertainty of 15% in the peak point at 0.55 Å and of only 10% at 1.0 Å from the line center.

A second correction involved a subtraction of the background signal level. (Calculations of the continuum emissivity at this wavelength from known plasma conditions indicated that approximately 90% of the background was due to scattered light of other wavelengths.) A measurement of this level was obtained at several points far removed from the line center on each side of the line and interpolated over the included band. The final results of this background correction for displacements from the line center greater than ±2 Å are shown dashed in Fig. 5. This technique permitted an ultimate profile determination over a

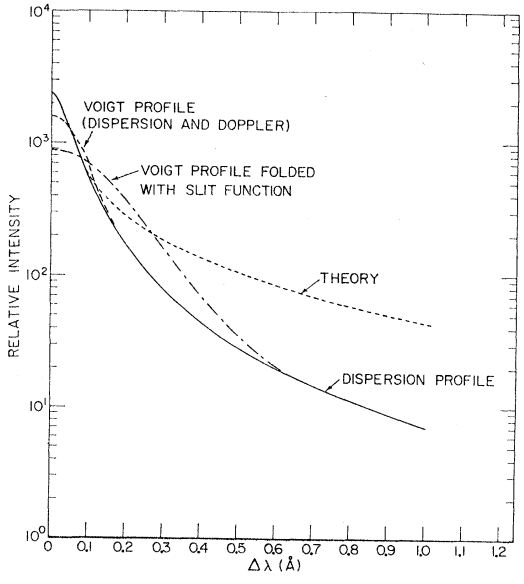

FIG. 6. Comparison of the theoretical Stark profile for Lyman-α with a dispersion profile fitted at $\Delta\lambda=0$, a normalized Voigt profile combining the dispersion and Doppler profiles, and a superposition of the Voigt profile and the slit function ($N_e=3.3\times10^{17}$ cm^{-3}, $T\approx20\,000$°K).

range of three decades in the emission coefficient for the Lyman-α line.

The full half-width of the Lyman-α line, as calculated from Stark-broadening theory for the conditions discussed, is 0.15 Å, while Doppler broadening due to the thermal motion of the radiating atoms gives a Gaussian profile with a full half-width 0.12 Å. Furthermore, the calculated theoretical Stark profile can be fitted quite well by a dispersion function below 0.15 Å, when normalized at the line center (Fig. 6). Using a Voigt function[24] to fold the Doppler profile into this dispersion profile, it was determined that the Doppler broadening exerted negligible influence on the dispersion profile beyond 0.2 Å (Fig. 6) and, therefore, had even less of an effect upon the theoretical Stark profile in the more slowly falling wings. We may carry this analysis a step further and fold in a rectangular slit function to account for the instrumental broadening. Again referring to Fig. 6, it is seen that the slit function produced negligible effects on the Voigt function for wavelengths greater than 0.55 Å from line center; and once again the effect upon the theoretical Stark profile is even less, i.e., negligible for wavelengths greater than 0.5 Å.

LYMAN-α PROFILE RESULTS

The experimental Lyman-α profile which evolved from the procedure described above is compared with the theoretically predicted profile over an intensity range of 1000 in Fig. 7. These data are plotted at a charged-particle density of $(3.3\pm0.3)10^{17}$ cm^{-3}, reproducible within 3% from point to point, and at a temperature of $\sim$20 000 °K, reproducible to better than 1%. Such reproducibility, especially with respect to temperature, accounts for the smooth experimental profile obtained by this technique as discussed previously. The theoretical profile (solid line) was calculated for the measured density and temperature throughout the region $|\lambda-\lambda_0|<2.5$ Å with an estimated numerical accuracy of 10% from calculations due to Griem, Kolb, and Shen,[5] which combined a generalized impact theory developed independently by Baranger[25] and by Kolb and Griem[26] for the electron effects with the quasistatic Holtsmark theory for ions corrected for correlation and shielding effects. For $|\lambda-\lambda_0|>2$ Å an asymptotic formula was used.[27] The Lewis correction[28] to the impact broadening was incorporated into this calculation, resulting in a theoretical wing profile in agreement at 2 and 7 Å from the line center with the results of a similar calculation neglecting both this effect and the so-called strong collision term, and with a maximum deviation in intensity of -10% at 4 Å and $+10\%$ at 12 Å (comparable to the estimated accuracy of the impact-theory calculations and the experimental uncertainties). This theoretical line shape is compared with the original Holtsmark theory[2,29] (shown dashed in Fig. 7) which only includes ion broadening on a quasistatic basis, without correlation or shielding effects.

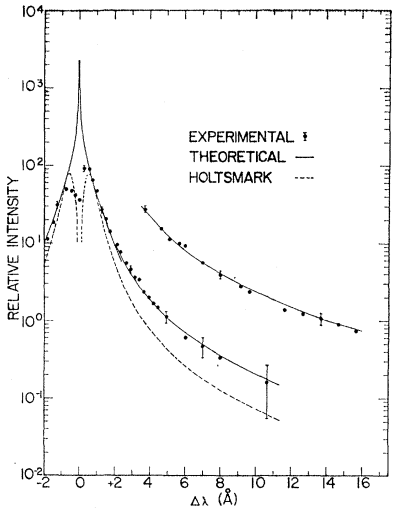

FIG. 7. Comparison of experimental and two calculated Stark profiles for Lyman-α. The more accurate experimental profile for the far wing was obtained at a higher hydrogen concentration. Estimated experimental errors are indicated on a few points ($N_e=3.3\times10^{17}$ cm^{-3}, $T\approx20\,000$°K).

The comparison between the experimental and the new theoretical profiles was effected by sliding the ordinate on a logarithmic scale to obtain a best fit over the wavelength interval 0.5 Å$<|\lambda-\lambda_0|<2$ Å in which the experimental data was particularly accurate and least affected by corrections. As a further precaution against small errors, the data plotted at each point in this zone represents an average over several shots during the profile scan. In addition, several critical points in this region were monitored before the scan was begun and also after its completion, as a check against systematic errors arising during the experiment. No alignment of the theoretical and experimental profiles was made along the wavelength axis since the center of the profile is not well defined, due to the asymmetrical absorption dip caused by boundary layer reabsorption effects for points within about 0.5 Å from line center. Indeed, the asymmetrical results shown in Fig. 7, as well as the relation of the line center to the position of the narrow line obtained at lower densities, seem to indicate a shift of the Lyman-α line towards longer wave lengths by about 0.2 Å.

A comparison with the Holtsmark theory was made by adjusting the Holtsmark profile so that the two

[24] H. C. van de Hulst and J. J. M. Reesinck, Astrophys. J. **106**, 121, (1947).
[25] M. Baranger, Phys. Rev. **111**, 481 (1958).
[26] A. C. Kolb, and H. Griem, Phys. Rev. **111**, 514 (1958).
[27] H. R. Griem, Astrophys. J. **136**, 422, (1962); see also U. S. Naval Research Laboratory Report NRL Report 5805, 1962 (unpublished).
[28] M. Lewis, Phys. Rev. **121**, 501 (1961).
[29] A. B. Underhill and J. H. Waddell, Natl. Bur. Std. Circ. **603** (1959).

theoretical profiles coincided near the line center at the point of equal slope (Fig. 7). Such a comparison led to a variation between theories on the far wings of the line by a factor of 3, whereas a comparison of (area) normalized profiles resulted in a wing factor of 2.

The second wing profile obtained at a higher hydrogen concentration from +4 to +16 Å is also shown in Fig. 7. It mainly served as an extrapolation of the data obtained on the first profile, with improved accuracy on the far wing as discussed above. Since the experimental results beyond 4 Å could be fitted quite well to either theoretical curve, no attempt was made to compare the theories for the second profile. Accurate measurements in the region $|\lambda-\lambda_0|<4$ Å (and in particular between 1 and 2.5 Å, where the results are not sensitive to the corrections employed) are therefore most essential in comparing the experimental results with the two theories, which suggested the normalization of the theoretical profiles in this region. (In experiments with different charged particle densities, the scaling with $N_e^{2/3}$ should be observed here.)

Measurements on an absolute scale (based upon the emissivity determinations) of the wing absorption coefficient were also consistent with a coefficient calculated using the more recent profile theory,[27] although limited to an accuracy of $\times 2$ (due chiefly to uncertainties in the plasma temperature determination).[30]

LYMAN-β PROFILE RESULTS

An experimental profile of the Lyman-β line was obtained much in the same way as for Lyman-α. Since, however, this line was considerably weaker, it was necessary to measure the complete profile at an initial hydrogen pressure of 0.040 mm Hg in order to have sufficient signal on the far wings of the line. The experimental results are compared with theory in Fig. 8 for the interval $|\lambda-\lambda_0|<6$ Å. As shown, there was considerably more interference on Lyman-β from impurity radiation, which produced excessively large fluctuations in signal beyond 6 Å from center so that the results beyond that limit were not included. Such impurity lines were useful, however, in serving as a gauge to check the scanning technique.

In order to obtain adequate signals on the line wing, both the Lyman-α and Lyman-β profiles were measured

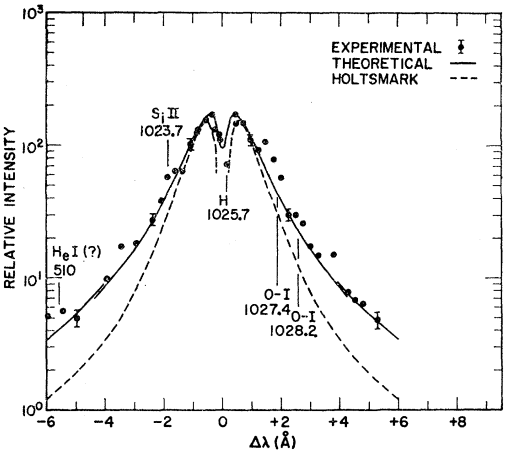

FIG. 8. Comparison of measured and two calculated Stark profiles for Lyman-β. Estimated experimental errors are indicated on a few points, as are the positions of the unperturbed Lyman-β line and various impurity lines ($N_e=3.0\times10^{17}$ cm^{-3}, $T\approx20\,000$°K).

with a resolution of 0.4 Å. Within this limitation, the dip in the center of Lyman-β corresponded quite well to the predicted theoretical dip for this line. Since an accurate measurement of the depth of the well in the true profile would provide a critical test of the ion-field distribution function employed in the theoretical calculations a more detailed study of this region using narrower slits, and consequently higher resolution (0.2 Å), was carried out at various hydrogen concentrations in order to study the depth and shape of the well and to possibly determine the extent of reabsorption effects. Concentration curves, i.e., graphs of signal strength versus total hydrogen concentration, were plotted from this data at several wavelengths throughout the central region in hopes that linear optically thin conditions might be found at low concentrations, thus indicating negligible reabsorption. Unfortunately, a central zone of about ±0.5 Å was somewhat optically dense even at the lowest concentrations, so that no definitive measurements accurate enough to aid in the identification of the proper field strength distribution function were possible.

One conclusion to be drawn from this data was an indication of a shift of ~0.2 Å towards shorter wavelengths (Fig. 8). The location of the unshifted line at 1025.7 Å was obtained from a previous calibration of the spectrograph and also by the signal shape at this wavelength. More specifically, photomultiplier signals from the wings of the spectral lines as well as from the visible continuum generally decayed in about 10 μsec, whereas the signal from a wavelength corresponding to the unshifted line showed a decay time greater than 50 μsec. An enhanced intensity at the unshifted line due to a narrowing of the spectral line as the charged-particle density decreased and to an increase in neutral hydrogen density as the temperature decreased behind the shock

[30] In a recent arc experiment [G. Boldt and W. S. Cooper (to be published)] the Lyman-α wing absorption coefficient has also been measured on an absolute scale and was found to be twice the theoretical Holtsmark value at large distances from the line center. However, the arc measurements could not be extended to as small a wavelength displacement from the line center as in the present experiment and also the electron density was smaller, both effects together resulting in an increase of the minimum value of $\alpha=\Delta\lambda/F_0$ by a factor of about 5. (Here F_0 is the Holtsmark field strength, $F_0=2.61eN_e^{2/3}$.) Therefore the arc experiment does not provide a sensitive check on the theoretically predicted slopes of the profiles, which differ significantly only at small displacements α as covered by the measurements described in the present paper.

front accounted for this anomaly in the time history of the signal.

SUMMARY

This experiment yielded a comparison of measured Stark profiles with the results of recent calculations as well as with the older Holtsmark results for the theoretically most fundamental case—the first resonance line of atomic hydrogen (Lyman-α). The line profiles were obtained by a shot-to-shot scan using an extremely reproducible T–type shock tube, specially designed for this experiment, as a light source. A similar measurement of the profile of the Lyman-β line further established the validity of the techniques used for Lyman-α. The charged particle density determined independently of line-broadening theory from an absolute measurement of the emitted continuum radiation gave results consistent with those obtained from a measurement of visible helium linewidths, as well as from a measurement of the incident shock velocity. Spectroscopic temperature measurements based upon a helium line-to-continuum ratio technique also gave results consistent with estimates from the hydrodynamic measurements. A sensitive check on the reproducibility, accomplished by monitoring the average shock velocity over the entire tube length, verified the excellent shot-to-shot reproducibility predicted by the sensitive intensity measurements in the vacuum ultraviolet spectral region. Information obtained from stereoscopic spectroscopic data supported the evidence obtained from streak photography of a sharp plane shock front, distinctly isolated from an impurity-dominated plasma cloud presumably originating in the arc region.

Detailed studies in which the hydrogen concentration was varied verified the optically thin source assumption on the line wing for low hydrogen concentrations and suggested a controlled approach to blackbody conditions at higher concentrations. The consistency between the measured and the calculated emissivity on the line wing, along with the flat-top profiles obtained for optically thick lines, added support to the association of the measured saturation level with the blackbody limit.

The results obtained for the wing of the Lyman-α line emitted from a uniform optically thin source, measured over an intensity range of 1000 and out to a wavelength distance of 100 times the half-width, clearly verify the validity of recent Stark broadening calculations[5,27] within $\sim$10%. Contrasted to the Holtsmark theory, the difference in slopes culminated in a factor of about three between the extreme wing intensities, when the profiles were normalized at the point of equal slope (near the line center). The conclusions to be drawn from Lyman-β are similar, although the evidence is less extensive. The shock tube developed for this experiment shows promise as a vacuum ultraviolet light source approaching blackbody conditions in a controlled fashion in defined wavelength intervals.

ACKNOWLEDGMENTS

The authors are indebted to J. L. Ford for his technical criticism and assistance in carrying out the experimental work. The numerous important contributions of A. C. Kolb and other members of the NRL Plasma Physics Branch are greatly appreciated.

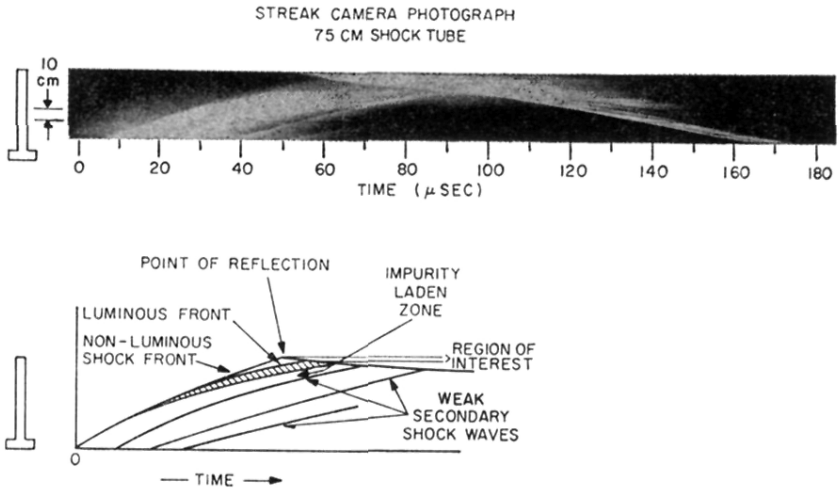

FIG. 2. Typical streak camera photograph of a portion of the 75-cm shock tube with the camera slit imaged parallel to the tube axis. The lower diagram identifies features more apparent on the original negative and, in particular, on similar photographs taken in color, where a red luminous zone and reflected shock wave were quite distinct when compared to the cooler impurity region (white) behind the interface.

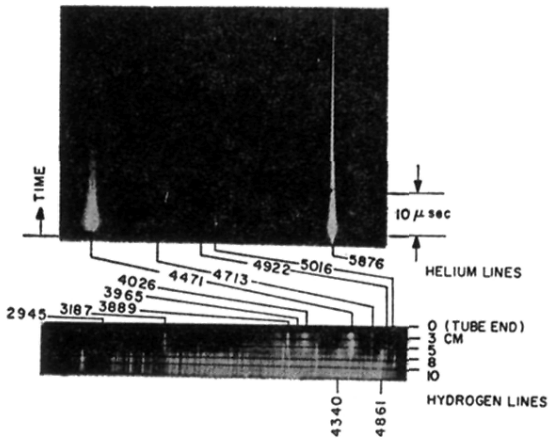

FIG. 3. Time-resolved (taken at 3 mm from reflector) and space resolved (along the major axis) spectra. (Radiation from the first centimeter behind the reflector is obscured on the latter spectrum by the vacuum sealant.) The horizontal dark lines are reference marks on the tube. Both spectra were obtained on single shots.